Current Biology 23, 1154–1162, July 8, 2013 ©2013 Elsevier Ltd All rights reserved http://dx.doi.org/10.1016/j.cub.2013.05.005

Article

Actin Filament Severing by Cofilin Dismantles Actin Patches and Produces Mother Filaments for New Patches

Qian Chen[1] and Thomas D. Pollard[1,2,3,*]
[1]Department of Molecular, Cellular, and Developmental Biology
[2]Department of Molecular Biophysics and Biochemistry
[3]Department of Cell Biology
Yale University, P.O. Box 208103, New Haven, CT 06520-8103, USA

Summary

Background: Yeast cells depend on Arp2/3 complex to assemble actin filaments at sites of endocytosis, but the source of the initial filaments required to activate Arp2/3 complex is not known.
Results: We tested the proposal that cofilin severs actin filaments during endocytosis in fission yeast cells using a mutant cofilin defective in severing. We used quantitative fluorescence microscopy to track mGFP-tagged proteins, including early endocytic adaptor proteins, activators of Arp2/3 complex, and actin filaments. Consistent with the hypothesis, actin patches disassembled far more slowly in cells depending on severing-deficient cofilin than in wild-type cells. Even more interesting, actin patches assembled slowly in these cofilin mutant cells. Adaptor proteins End4p and Pan1p accumulated and persisted at endocytic sites more than ten times longer than in wild-type cells, followed by slow but persistent recruitment of activators of Arp2/3 complex, including WASP and myosin-I. Mutations revealed that actin filament binding sites on adaptor proteins Pan1p and End4p contribute to initiating actin polymerization in actin patches.
Conclusions: We propose a "sever, diffuse, and trigger" model for the nucleation of actin filaments at sites of endocytosis, whereby cofilin generates actin filament fragments that diffuse through the cytoplasm, bind adaptor proteins at nascent sites of endocytosis, and serve as mother filaments to initiate the autocatalytic assembly of the branched actin filament network of each new patch. This hypothesis explains the source of the "mother filaments" that are absolutely required for Arp2/3 complex to nucleate actin polymerization.

Introduction

Assembly of actin plays a key role in clathrin-mediated endocytosis in yeast by providing both scaffold for the membrane invagination and force for scission of the vesicle against turgor pressure [1–3] (for review see [4, 5]). The sites of endocytosis are called actin patches.

Genetics and quantitative fluorescence microscopy provided many details about the molecular composition and assembly pathway of actin patches, including evidence that Arp2/3 complex nucleates the actin filaments [6–8], but questions remain about every stage of the process. Biochemical studies showed that Arp2/3 complex must bind both a nucleation-promoting factor (NPF) and a preexisting filament to initiate a new filament [9]. However, the source of these mother filaments is unclear in fungi [7]. An immediately adjacent actin patch can be a source of actin filaments [10], but most patches form in regions of cortex apparently devoid of actin filaments [11]. However, electron microscopy of animal cells suggested that actin filaments may be present at sites of endocytosis earlier than indicated by fluorescence microscopy [12]. Questions also remain about disassembly of the actin coat. Simulations of a mathematical model of fission yeast endocytic patches demonstrated that dissociation of subunits from the ends of actin filaments is too slow to account for disappearance of the filaments in 10 s, unless the filaments are severed into fragments small enough to diffuse out of the patch and disassemble elsewhere [7]. Dissociation of Arp2/3 complex from the branched actin filaments has been proposed as a mechanism [13], and while cofilin stimulates debranching [14], this reaction was not necessary to account for the turnover of filaments in patches [7].

The small protein cofilin severs actin filaments [15–17] and contributes to many processes, including endocytosis, cell motility, and cytokinesis [18–20]. Cofilin concentrates in yeast endocytic actin patches [21–23], and cofilin mutations cause endocytic defects [19, 21, 23].

Here we used a mutant cofilin with a selective defect in severing [18] to study how actin filament severing contributes to endocytosis in fission yeast. Endocytic actin patches disassembled very slowly in mutant cells, as anticipated by studies in budding yeast [21, 23]. Surprisingly, actin patch assembly took longer in cofilin mutant cells, with prolonged accumulation of both membrane adaptor proteins and activators of Arp2/3 complex before assembly of actin. Depletion of the actin monomer pool could not explain these defects in cofilin mutant cells. Instead, we present evidence to support a feedback mechanism where severing by cofilin generates short actin filaments that interact with endocytic adaptor proteins End4p and Pan1p and Arp2/3 complex to initiate actin polymerization at sites of endocytosis.

Results

Cofilin Concentrates in Actin Patches

We studied the localization of cofilin in fission yeast by expressing cofilin tagged on the N terminus with mGFP (Figure 1A; see also Figure S1A available online). The protein is the product of the *adf1*$^+$ gene, but we use the common name, cofilin or mGFP-cofilin, because *adf1*, actin-depolymerizing factor 1, is a misleading name for a protein that does not depolymerize actin filaments [15–17]. This fusion protein must be overexpressed from either the *adh1* (alcohol dehydrogenase 1) or the strong *3nmt1* promoter to complement a *Δadf1* null mutation [18, 22]. The *adf1::Padh-mGFP-adf1* cells expressed about 10-fold more mGFP-Adf1p than Adf1p in the *adf1*$^+$ cells (Figure S1B). These cells grew normally at both 25°C and 30°C but slightly more slowly at 36°C, compared to wild-type cells (Figure S1C). After correcting for excluded volume [24], the total fluorescence in *adf1::Padh-mGFP-adf1* cells corresponded to a cytoplasmic concentration of 200 μM mGFP-cofilin.

*Correspondence: thomas.pollard@yale.edu

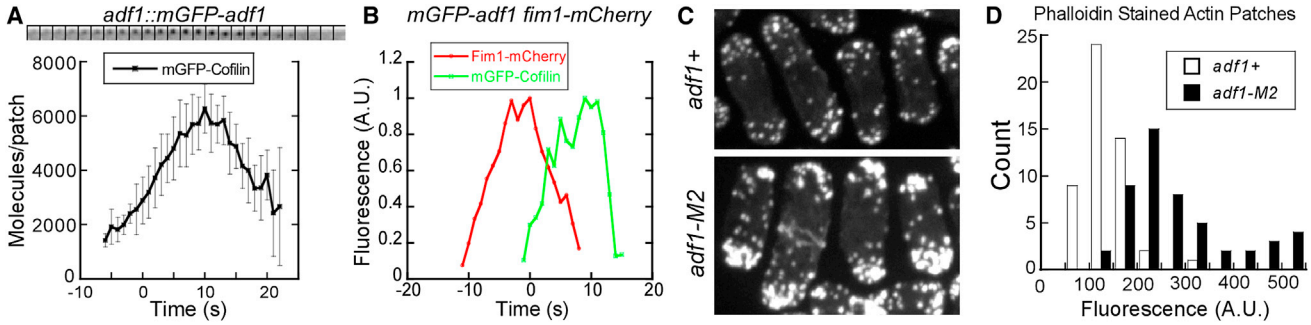

Figure 1. Cofilin Localization in Endocytic Actin Patches of Fission Yeast Cells and Effects of a Cofilin Mutation that Reduces Severing on Actin Filament Accumulation in Patches

(A) Time course of mGFP-cofilin in actin patches. Upper panel shows a time series of negative-contrast fluorescence micrographs of an actin patch at 1 s intervals. Images are sums of five median slices of the cell. Lower panel shows a graph of the average number of molecules of mGFP-cofilin per patch (±SD) over the time.

(B) Time courses of normalized fluorescence intensities of mGFP-cofilin (green) and Fim1p-mCherry (red) in one actin patch. See also Figure S1.

(C and D) Comparisons of actin patches in wild-type *adf1*$^+$ and cofilin mutant *adf1-M2* cells. Maximum-intensity projections of z series of fluorescence micrographs of *adf1*$^+$ cells and *adf1-M2* cells fixed and stained with rhodamine-phalloidin for actin filaments are shown in (C). Histogram of fluorescence intensities of 50 actin patches from *adf1*$^+$ (open) and *adf1-M2* (black) cells are shown in (D). See also Figure S1.

We used two-color fluorescence microscopy to compare mGFP-cofilin with either End4p-mCherry, an early endocytic adaptor protein, or Fim1p-mCherry, the fission yeast homolog of the actin filament binding protein fimbrin (Figures 1B and S1D). Actin patches in cells depending on overexpressed mGFP-cofilin assembled and disassembled Fim1p-mCherry normally (Figure S1E), and the lifetime of End4p increased only slightly from 36 s to 39 s (n = 20). mGFP-cofilin appeared at sites of endocytosis 5 s before actin patches began to move from the cell surface (defined as time zero), peaked at 6,000 molecules at time +10 s, and then gradually dissipated over the next 10 s (Figure 1A). The mGFP-cofilin fluorescence peaked after both End4p and Fim1p and persisted after both proteins dissociated from moving patches (Figures 1B and S1D).

Endocytic Defects in Cofilin Mutant *adf1-M2* Cells

To study the role of cofilin during endocytosis, we used cells depending on mutant cofilin-M2, which binds and severs actin filaments far more slowly than the wild-type cofilin [18]. Fission yeast *adf1-M2* cells have larger diameters than the wild-type cells, similar to many other endocytic mutants [25]. Calcofluor white stained the cell walls more intensely in these mutant cells than in wild-type cells (data not shown), a defect observed in other endocytic mutants. The average fluorescence intensity of actin patches stained by rhodamine-phalloidin was 2-fold greater in *adf1-M2* cells (281 ± 107, n = 50) than in wild-type cells (139 ± 42, n = 50) (Figures 1C and 1D). During interphase, these bright actin patches packed more densely at the poles of cofilin mutant cells than in wild-type cells (Figure 1C).

We looked for endocytic defects in the *adf1-M2* cells using two approaches: (1) localization of the fission yeast homolog of the SNARE protein synaptobrevin Syb1p (Figure S2F) and (2) pulse-chase experiments with the fluorescent lipophilic dye FM4-64 (Figure S2G). After exocytosis, Syb1p recycles from the plasma membrane through the endocytic pathway, a process compromised by many endocytic mutations in both budding and fission yeast [10, 26]. GFP-Syb1p concentrated in numerous cytosolic puncta in both wild-type and *adf1-M2* cells but associated mostly with the plasma membrane in *adf1-M2* cells (Figure S2F), consistent with defects in endocytosis. Pulse-chase experiments confirmed that *adf1-M2* cells internalized FM4-64 very slowly. Wild-type cells took up FM4-64 from the plasma membrane into numerous cytoplasmic puncta in <8 min (Figure S2G), but after 16 min most of the dye remained on the surface of *adf1-M2* cells with very few fluorescence puncta in the cytoplasm (Figure S2G).

Defects in Actin Patch Assembly and Disassembly in Cofilin Mutant *adf1-M2* Cells

We used quantitative fluorescence microscopy to compare actin patch dynamics of wild-type and *adf1-M2* cells expressing six endocytic proteins tagged with mGFP (Figures 2 and S2A). We aligned time courses of all actin patches based on their initial inward movement (time zero). As in budding yeast [4, 8], fission yeast initiate endocytosis by sequentially recruiting clathrin, adaptor proteins, NPFs for Arp2/3 complex, and finally Arp2/3 complex itself [6]. We tracked two adaptor proteins, End4p/Sla2p (a homolog of Hip1r [27]) and Pan1p (an Eps15 protein [28]). We also tracked NPFs, the homolog of Wiskott-Aldrich syndrome protein (Wsp1p), and myosin-I (Myo1p), which stimulate Arp2/3 complex to initiate the explosive assembly of actin filaments [7, 25, 29, 30] in cooperation with the F-BAR proteins [31]. We tracked actin filaments with either Fim1p-mGFP expressed from its genomic locus or mGFP-Act1p (mGFP-actin) expressed at a low level from the *leu1* locus under the control of a suppressible *41nmt1* promoter in cells with a wild-type actin gene.

Actin patches in *adf1-M2* cells accumulated mGFP-actin at the same rate as wild-type cells, but the accumulation phase lasted three times longer (30 s versus 10 s) (Figure 2B), so the peak number of mGFP-actin molecules per actin patch was 3-fold higher in cofilin mutant cells than in wild-type cells (Figure 2B), confirming the more intense staining with rhodamine-phalloidin (Figure 1C). Nevertheless, these actin patches in *adf1-M2* cells accumulated the normal amount of the actin-binding protein Fim1p-mGFP but more slowly than wild-type cells (Figure 2A). After time zero, mGFP-actin and Fim1p-mGFP took about 10 s to disappear from patches in wild-type cells (Figure 2A), but both proteins persisted far longer in *adf1-M2* cells, taking as long as 180 s to completely disappear from some patches (Figure 2A). In many cases, these

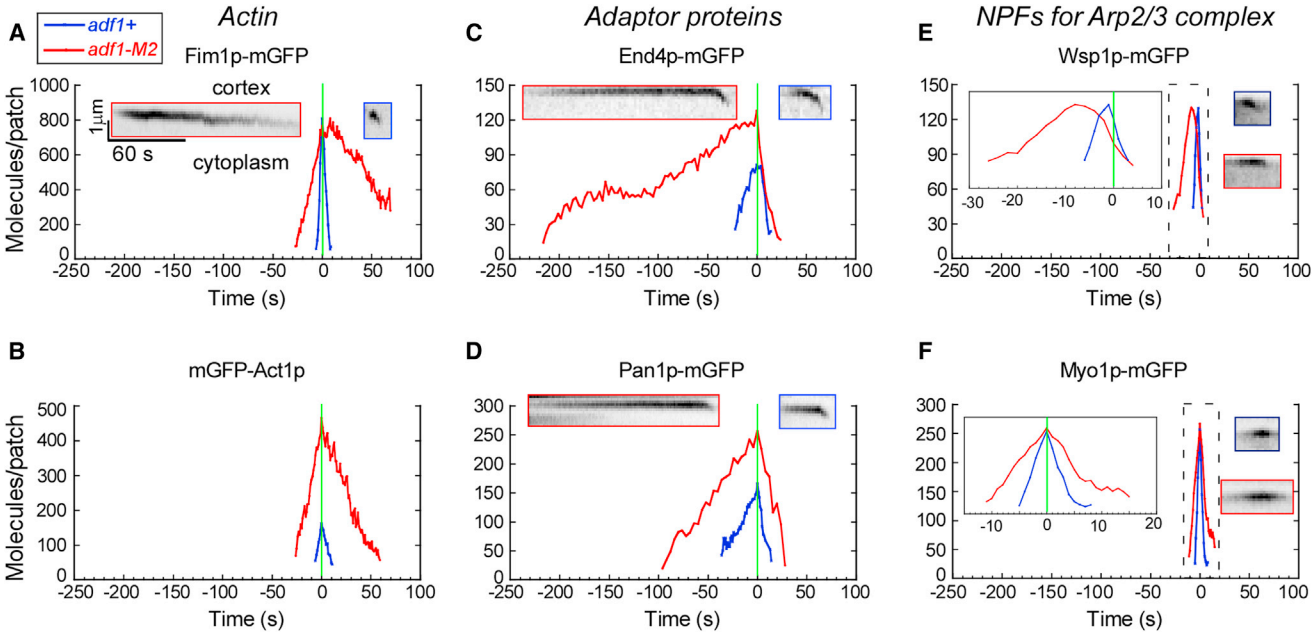

Figure 2. Accumulation and Disappearance of Fluorescent Proteins in Actin Patches

Time courses of the accumulation and disappearance of fluorescent proteins in actin patches of wild-type *adf1*$^{+}$ cells (blue lines) and cofilin mutant *adf1-M2* cells (red lines). Graphs show the average number of molecules at each point in time. Data from individual patches were aligned at the time they started to move (time zero, green line). Inserts are kymographs of fluorescence micrographs of individual actin patches in wild-type cells (blue outline) or *adf1-M2* cells (red outline). Inserts in (E) and (F) are expanded timescales for data in dashed boxes. Shown are Fim1p-mGFP (A), mGFP-Act1p (B), End4p-mGFP (C), Pan1p-mGFP (D), mGFP-Wsp1p (E), and mGFP-Myo1p (F). See also Figure S2.

persisting actin patches in *adf1-M2* cells moved from their initial locations, and occasionally they appeared to merge with nearby actin patches.

Quantitative microscopy revealed that the early stages of actin patch assembly were prolonged in *adf1-M2* cells (Figures 2C and 2D). Two adaptor proteins, End4p-mGFP and Pan1p-mGFP, appeared at actin patches around time −30 s in wild-type cells, but both appeared before −100 s in *adf1-M2* cells and accumulated to higher levels than in wild-type cells (Figures 2C and 2D). Prolonged accumulation of End4p and Pan1p resulted in ~1.5-fold more of these adaptors in actin patches (Figure 3A) at the time NPFs arrived prior to actin polymerization. Imaging actin patches in *adf1-M2* and wild-type cells side by side confirmed the presence of more End4p-mGFP in the long-lived actin patches of the mutant cells (Figure 3B), as observed by quantitative fluorescence imaging. The NPFs Wsp1p and Myo1p also accumulated more slowly in the actin patches of *adf1-M2* cells than in wild-type cells (Figures 2E and 2F), but the cofilin mutation did not alter their peak numbers (Figure 3A). Both membrane adaptor proteins dissociated from actin patches in 20 s in *adf1-M2* cells, slightly more slowly than in wild-type cells (10 s) (Figures 2C and 2D). The movements of patches away from the cell surface were indistinguishable in *adf1-M2* and wild-type cells (Figure S2B). Similarly, both NPFs disappeared slightly more slowly than normal from patches in *adf1-M2* cells. We used two-color fluorescence microscopy of live cells expressing a tagged adaptor protein and either Myo1p or Fim1p to confirm the timing of these events (Figures 3C–3F).

Thus, defective actin filament severing in *adf1-M2* cells not only slowed disassembly of actin patches (as expected) but also prolonged the accumulation of adaptor proteins and NPFs, delaying the initiation of actin filament assembly in actin patches, a defect that we confirmed in cells depending on the mutant cofilin-M3 with a slightly milder defect in severing actin filaments (Figures S2C and S2D) [18]. We considered two mechanisms that might explain these assembly defects: (1) depletion of the cytoplasmic pool of actin monomers and (2) a deficiency of actin filament fragments to stimulate Arp2/3 complex in adjacent actin patches.

Depletion of Actin Monomers Does Not Mimic the Defects in Actin Patch Assembly of Cofilin Mutant Cells

We investigated whether slow severing and depolymerization of actin filaments in *adf1-M2* cells might deplete the cytoplasmic pool of actin monomers, leading secondarily to defects in actin patch assembly. A shortage of actin monomers would not only slow nucleation and elongation of actin filaments but also might compromise binding of Arp2/3 complex to mother filaments [32].

Quantitative fluorescence microscopy of cells expressing mGFP-actin from the *41nmt1* promoter in the *leu1* locus showed that the cytoplasmic mGFP-actin fluorescence was 10% lower in a*df1-M2* cells than in wild-type cells (Figure S2E). To test whether this slightly lower pool of cytoplasmic actin might cause endocytic defects in *adf1-M2* cells, we studied actin patches in wild-type cells treated with latrunculin A (LatA), a small molecule that binds actin monomers with high affinity and inhibits polymerization [33–35]. At 8 μM, LatA increased the cytoplasmic fluorescence of mGFP-actin ~30% (Figure S2F). We interpret this change to be sequestered mGFP-actin bound to LatA. This effect of LatA on the pool of unpolymerized actin available to assemble actin patches should be sufficient to mimic the 10% smaller amount of cytoplasmic actin in *adf1-M2* cells.

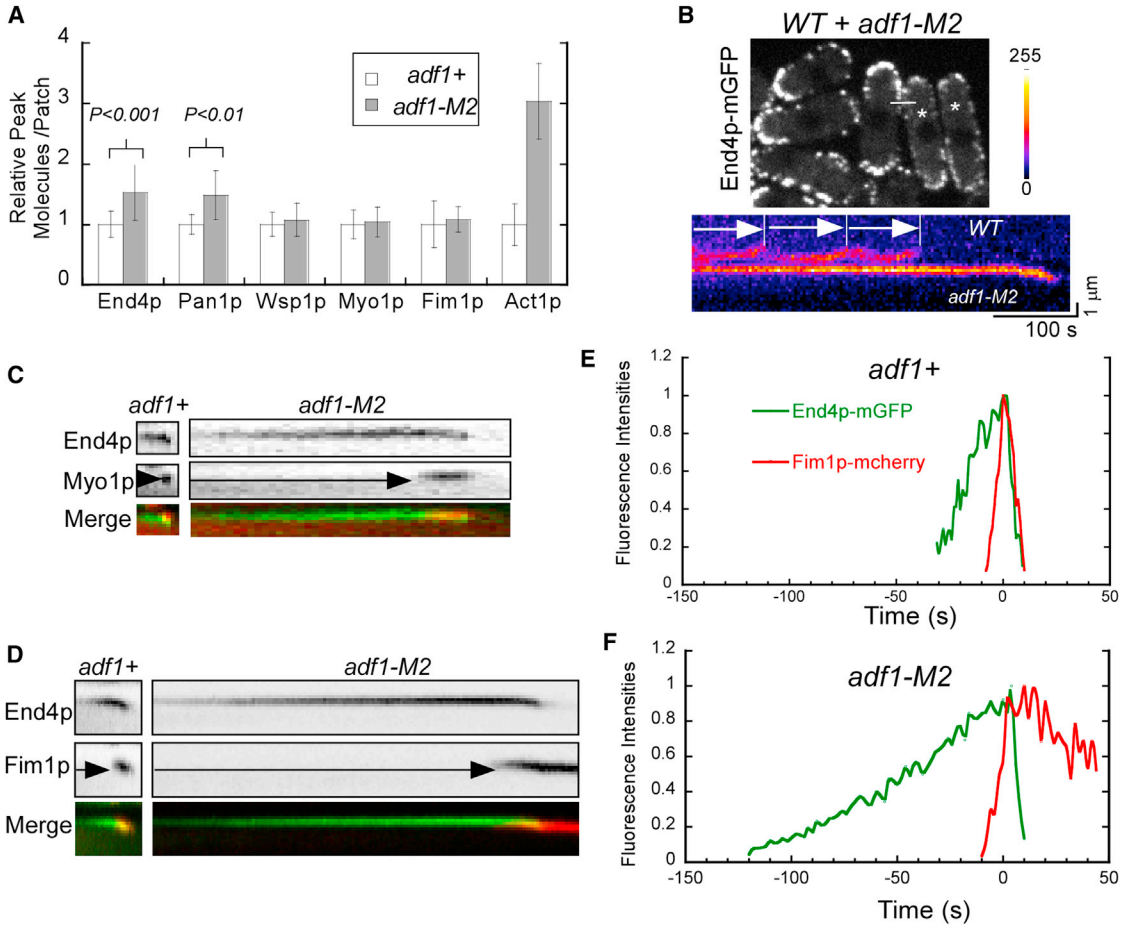

Figure 3. Accumulation of Endocytic Adaptor Proteins in Actin Patches of Wild-Type and Cofilin Mutant Cells before Actin Assembly

(A) Histogram of peak numbers of proteins per actin patch in wild-type *adf1*$^+$ cells (open bars) and cofilin mutant *adf1-M2* cells (shaded bars). Mean numbers ± SD are normalized against wild-type actin patches. p values are from two-tailed Student's t tests.

(B) Side-by-side comparison of actin patches in wild-type (asterisk) and *adf1-M2* cells expressing End4p-mGFP. Top panel shows a fluorescence micrograph (sum of five middle z slices of the cells) of a mixed population of cells. Wild-type cells were identified by expression of Fim1p-mCherry. Data for the kymograph were collected along the white line. Bottom panel shows a kymograph of pseudocolored fluorescence micrographs of actin patches in a pair of neighboring cells showing three actin patches (arrows) in the wild-type cell top and one prolonged actin patch in the *adf-M2* cell bottom.

(C and D) Kymographs of fluorescence micrographs of actin patches in wild-type *adf1*$^+$ (left) and *adf1-M2* (right) cells expressing pairs of fluorescent proteins, either End4p-mYFP and mCFP-Myo1p (C) or End4p-mGFP and Fim1p-mCherry (D). Bottom panels are merged images with End4 (in green) and Myo1p/Fim1p (in red). Arrows designate the interval between the appearance of End4p and Myo1p/Fim1p in the patches.

(E and F) Time courses of normalized fluorescence intensities of End4p-mGFP (green) and Fim1p-mCherry (red) in actin patches of wild-type *adf1*$^+$ (E) and *adf1-M2* cells (F).

See also Figure S2.

Low concentrations of LatA (0–8 μM) prolonged the accumulation of both End4p-mYFP and mCFP-Myo1p in patches (Figures S2F–S2H). However, LatA only led to a small delay in the interval between the appearance of End4p and Myo1p in actin patches of wild-type cells (Figures S2F–S2H), as observed in *adf1-M2* cells (Figure 3). Furthermore, low concentrations of LatA inhibited the inward movement of actin patches, a defect not observed in cofilin mutant cells. For example, most actin patches (nine out of ten) failed to move inward in cells treated with 8 μM LatA. Therefore, sequestering a fraction of the pool of monomeric actin with LatA did not replicate the phenotype of cofilin mutant cells.

Roles of End4p and Pan1p in Initiating Actin Polymerization in Actin Patches

A second hypothesis to explain the defects in actin patch assembly in cofilin mutant cells is that the process depends on short actin filaments normally severed by cofilin from endocytic patches to serve as mother filaments to activate Arp2/3 complex. We also considered the possibility that proteins recruited early in the endocytic pathway might tether these filaments and enhance their impact. Among the proteins that join clathrin early in the endocytic pathway [6, 8], Pan1p and End4p are known to bind actin filaments [36, 37], making them candidates to retain diffusing actin filaments at endocytic sites before the arrival of NPFs and Arp2/3 complex. Eps15 homolog Pan1p [28] is essential in fission yeast (Figure S3A). End4p is a nonessential homolog of budding yeast Sla2p and animal Hip1r [27, 38]. Actin patches in *Δend4* cells formed elongated tails as they moved from the cell surface (Figure S3D), similarly to *Δsla2* deletion mutations in budding yeast [8].

Biochemical experiments showed that fission yeast Pan1p binds actin filaments like budding yeast Pan1p [39]. Pan1p has a conserved WH2 (W) motif, located at the very C terminus

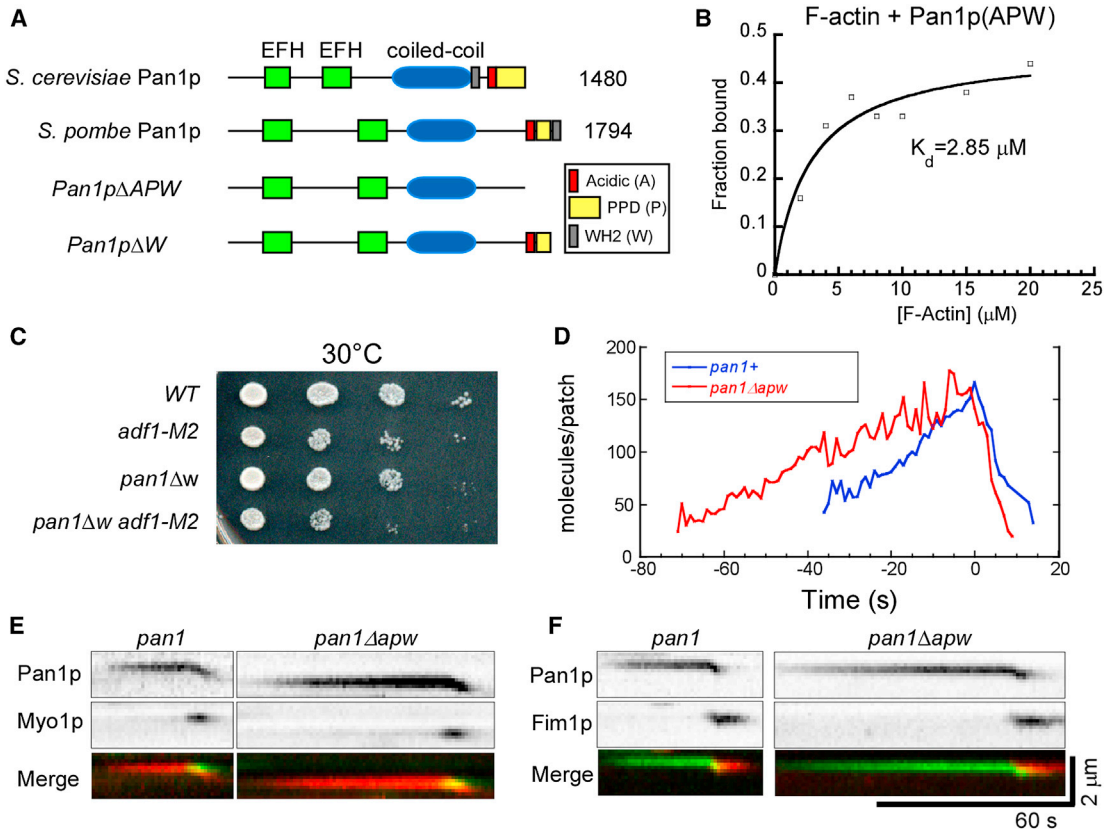

Figure 4. Analysis of Pan1p Binding to Actin Filaments and Effects of Deleting the Actin-Binding Region of Pan1p on Actin Patches

(A) Domain structures of budding yeast and fission yeast Pan1p (numbers are total amino acid residues) and Pan1p truncation mutants.

(B) Graph of the dependence of the fraction of $Pan1_{1633-1794}$ pelleted on the concentration of actin filaments. Samples of 2 μM $Pan1_{1633-1794}$ with 0–20 μM actin filaments were incubated at room temperature for 30 min in KMEI buffer before pelleting at 212,300 × *g* for 40 min. A bimolecular binding isotherm fit the data well with a K_d of 2.9 μM. Only 40% of GST-$Pan1_{1633-1794}$ (APW) was depleted from the supernatant with 20 μM actin, indicating that much of the protein was inactive.

(C) Viability of strains with the *pan1Δw* truncation mutation, *adf1-M2* mutation, or both mutations, measured by the growth of the dilution series for 2 days at 30°C.

(D) Time course of average number of molecules of Pan1p-mGFP (n = 10) or Pan1pΔW-mGFP (n = 12) per actin patch.

(E and F) Kymographs of fluorescence micrographs of actin patches from cells expressing wild-type or mutant Pan1p. The cells expressed Pan1pΔAPW-tdTomato and mGFP-Myo1p (E) or Pan1pΔAPW-mGFP and Fim1p-mCherry (F).

See also Figure S3.

after acidic (A) and polyproline (PP) motifs (Figures 4A and S3B). A purified C-terminal fragment of Pan1p ($Pan1p_{1633-1974}$), including the A, PP, and W domains, bound muscle actin filaments with a K_d of about 3 μM (Figure 4B), although only 40% of the GST-tagged protein was active.

We tested the effects on actin patch dynamics of two Pan1p truncation mutants designed to compromise binding to actin filaments. We deleted either the W domain alone in *pan1Δ1743-1794* (*pan1Δw*) or the A, PP, and W domains altogether in *pan1Δ1643-1794* (*pan1Δapw*) (Figure 4A). Cells expressed the *pan1* truncation mutant proteins at levels similar to full-length Pan1p (Figure S3C). Both mutations had negative genetic interactions with the *adf1-M2* mutation, with double mutants growing more slowly than the wild-type cells at 30°C (Figure 4C). Pan1pΔAPW-mGFP took twice as long as full-length Pan1p-mGFP to accumulate to normal levels in actin patches but dissociated from actin patches over the same time course as full-length Pan1p-mGFP (Figure 4D). The behavior of Pan1pΔW-mGFP was similar (data not shown). Strains depending on these *pan1* truncation mutants took ~40 s longer than wild-type cells to recruit Myo1p to actin patches (Figure 4E), so actin polymerization was delayed (Figure 4F). Similarly the interval between the appearances of End4p and Myo1p was longer in actin patches of *pan1* truncation mutants than in wild-type cells (data not shown). Therefore, the WH2 domain of Pan1p contributes to the initiation of actin patch assembly but is not essential.

We tested the effects on actin patch dynamics of two End4p truncation mutants designed to compromise binding to actin filaments. The C-terminal talin-like (TL) domain (also called an I/LWEQ domain) of budding yeast End4p can bind actin filaments [36, 40], but removing the TL domain had no detectable effect on the assembly of actin patches [40]. Using homology-based structural prediction ("Protein Homology/analogY Recognition Engine," http://www.sbg.bio.ic.ac.uk/phyre2), we found that the End4p sequence between the central coiled-coil and C-terminal TL domain has a high degree of sequence homology to the actin filament binding domain of talin (Figure 5A). This previously unrecognized TL domain may have compensated for deletion of the C-terminal TL domain in previous work. To compromise actin filament binding of End4p, we deleted either the C-terminal TL domain

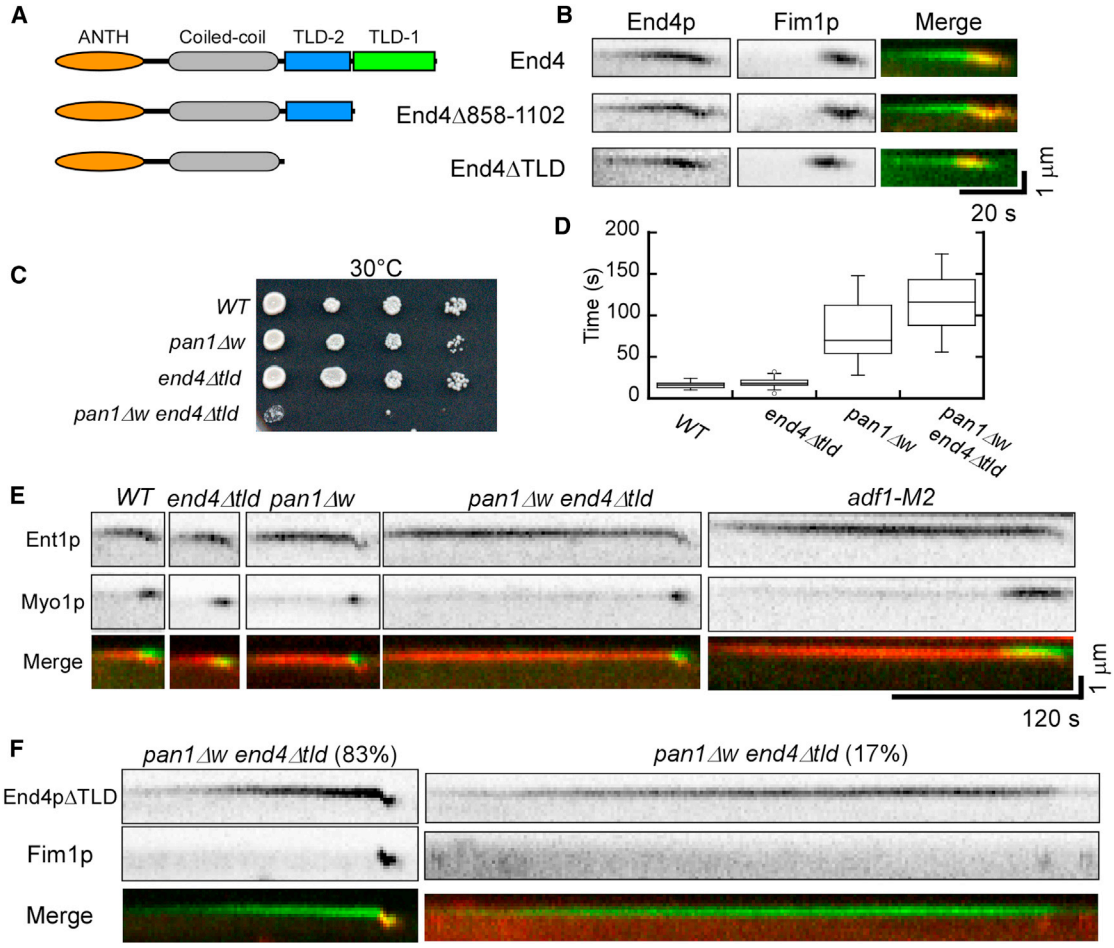

Figure 5. Actin Filament Binding Domains of End4p and Pan1p Cooperate to Initiate Actin Polymerization in Endocytic Patches

(A and B) Deletion of one or both talin-like domains from End4p. Domain structure of End4p and the two truncation mutants are shown in (A). Kymographs of fluorescence micrographs of actin patches in cells expressing either End4p or End4p truncation mutants tagged with mGFP and Fim1p-mCherry are shown in (B).

(C) Viability of strains with the *pan1Δw* mutation, *end4Δtld* mutation, and both mutations (*pan1Δw end4Δtld*), measured by growth of dilution series for 2 days at 30°C.

(D) Box plot of the time interval between the appearances of Ent1p and Myo1p in actin patches of wild-type, *end4Δtld*, *pan1Δw*, and *end4Δtld pan1Δw* cells. Horizontal lines in the boxes are average values. The boxes include ±25% from the average values. Vertical lines mark minimum and maximum values, except for outliners.

(E) Kymographs of fluorescence micrographs of actin patches in the wild-type, *end4Δtld*, *pan1Δw*, *end4Δtld pan1Δw* double mutant, and *adf1-M2* cells expressing both Ent1p-Tdtomato (top panels) and mGFP-Myo1p (bottom panels). The bottom panels are merged kymographs with Ent1p (in red) and Myo1p (in green).

(F) Kymographs of fluorescence micrographs of actin patches in *end4Δtld pan1ΔW* cells expressing End4pΔTLD- mGFP (top panels) and Fim1p-Tdtomato (bottom panels). Bottom panels are merged kymographs with End4pΔTLD (in green) and Fim1p (in red). Recruitment of Fim1p (left) was delayed in 83% of patches and failed in 17% of patches (right).

See also Figures S3 and S4.

(*end4Δ858-1102*) or both TL domains (*end4Δ663-1102*/*end4Δtld*) (Figure 5A).

Both *end4* TL domain deletion mutations had negative, temperature-sensitive interactions with the cofilin mutation *adf1-M2* (Figure S3E). mGFP-End4p lacking one or both TL domains was expressed at the same level as the full-length protein (Figure S3F), and it accumulated in and disappeared from actin patches normally (Figures S3G and S3H). Both *end4* mutant strains initiated actin assembly without delay (Figure 5B).

The *end4* mutants lacking TL domains had strong negative genetic interactions with *pan1* mutants lacking the WH2 motif (Figure 5C). The double mutant *pan1Δw end4Δtld* was temperature sensitive, growing very slowly at 30°C (Figure 5C) and dead at 36°C. On the other hand, the function of the newly identified actin filament binding motif of the fission yeast homolog of Epsin (Ent1p) [41] did not overlap with those of Pan1p (Figure S4 and Supplemental Results). The *pan1Δw end4Δtld* cells took up FM4-64 much more slowly than wild-type cells, even at the permissive temperature of 25°C. Wild-type cells took up most of the cell surface FM4-64 in less than 9 min, but most of the dye remained on the cell surface of double-mutant cells after 15 min (Figure S3I).

We observed endocytic adaptor protein Ent1p-tdTomato and mGFP-Myo1p to confirm that serious defects in actin patch assembly compromise endocytosis in *pan1Δw end4Δtld* double-mutant cells (Figures 5D and 5E). Ent1p normally

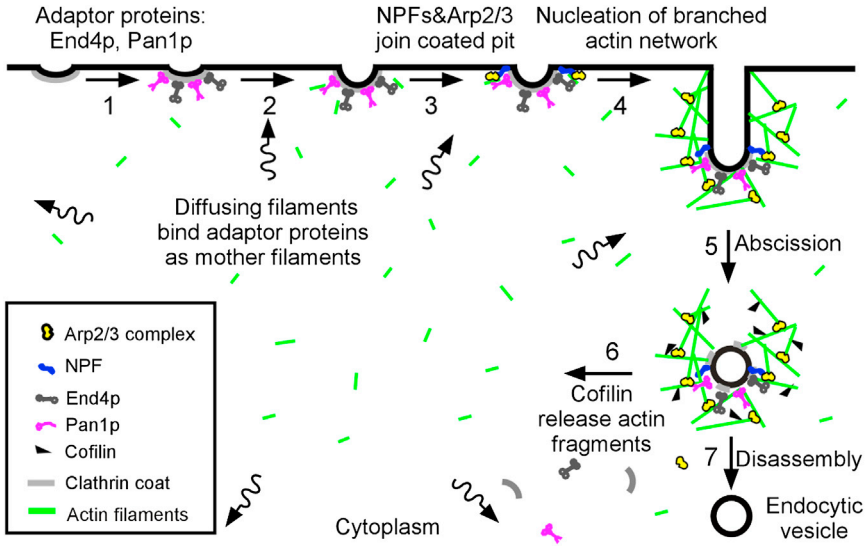

Figure 6. "Sever, Diffuse, and Trigger" Model for Actin Filament Turnover in Actin Patches

The seven steps (numbers next to the arrows) are: (1) Clathrin-coated pits bind adaptor proteins End4p and Pan1p. (2) Short, diffusing actin filaments bind to End4p and Pan1p associated with coated pits. (3) Arp2/3 complex interacts with these mother filaments and nucleation-promoting factors to (4) initiate branching nucleation of actin filaments that promote elongation of the endocytic tubule. (5) After abscission of the vesicle, (6) cofilin severs actin filaments to (7) disassemble actin patches and generate a pool of short, diffusing actin filaments, some of which return to the cycle at step 2.
See also Figure S5.

appears in actin patches ~30 s before initiation of actin assembly. The interval between the appearances of Ent1p and Myo1p in actin patches was 15.6 ± 3.9 s (n = 20) in wild-type cells, 19.6 ± 5.8 s (n = 30) in *end4Δtld* cells, 81.9 ± 35.2 s (n = 30) in *pan1Δw* cells, and 122.3 ± 55.8 s (n = 31) in *end4Δtld pan1Δw* double-mutant cells at the permissive temperature (Figure 5D). Actin patches in *adf1-M2* cells also recruited Myo1p slowly (Figure 2F). Actin assembly followed with Fim1p-mCherry was severely compromised in the double-mutant cells, with 17% (n = 30) of actin patches failing to recruit Fim1p-mCherry and initiate actin polymerization (Figure 5F). The patches in the double-mutant cells that polymerized actin did so with an average of 140 ± 62 s (n = 25) between the appearance of End4p and Fim1p compared with just 25 s in wild-type cells (Figure 5F).

Although we did not detect small actin filaments diffusing from patches in cells expressing mGFP-Lifeact (explained in Supplemental Results), we found that the depletion of actin filaments in cells by LatA inhibited recruitment of Arp2/3 complex and Myo1p at sites of endocytosis without preventing the accumulation of both End4p and Wsp1p (Figure S5 and Supplemental Results).

Discussion

Our experiments with a cofilin mutant defective in severing actin filaments confirmed that actin filament severing not only is essential for disassembling actin filaments in endocytic patches but also contributes to the assembly of actin patches. We attribute the endocytic defects of *adf1-M2* cells to slow severing by the mutant cofilin. Although the affinity of cofilin-M2 for actin filaments is 5-fold lower than wild-type cofilin, cooperative binding allows 2 μM cofilin-M2 to saturate 1 μM actin filaments [18], so cofilin-M2 will bind actin filaments but sever them slowly in the mutant cells. The effects of truncation mutations of two endocytic adaptor proteins support the proposal that cofilin produces short actin filaments that bind adaptor proteins and serve as primers to initiate actin polymerization at the site of endocytosis.

Actin Filament Severing by Cofilin Disassembles Endocytic Actin Patches

Disassembly of endocytic actin patches depends on cofilin in budding yeast [8, 21, 23], and our experiments demonstrate that the serving activity of cofilin is required (step 6, Figure 6). Slow binding of the mutant cofilin to actin filaments should also slow dissociation of branches [14] and may contribute to the slow turnover of patches. Since the cofilin mutation had little effect on the movement of actin patches (Figure S2B), neither scission of endocytic vesicles from the plasma membrane (step 5) nor vesicle movements appear to depend on disassembly of actin filaments. Membrane adaptor proteins and NPFs dissociated normally from actin patches (step 7), so these events are also independent of actin filament severing.

A "Sever, Diffuse, and Trigger" Hypothesis Explains the Cofilin Requirement for Actin Patch Assembly

Our most important finding is that the early steps in the assembly of actin patches depend on both actin filament severing by cofilin and actin filament binding by early endocytic adaptor proteins. These two seemingly disparate features suggest a "sever, diffuse, and trigger" hypothesis (Figure 6): cofilin generates actin filament fragments that diffuse through the cytoplasm (step 6), bind adaptor proteins at nascent sites of endocytosis (step 2), and serve as mother filaments (step 3) to initiate the autocatalytic assembly of the branched actin filament network of each new patch (step 4). This hypothesis offers one feasible explanation for the source of mother filaments that are absolutely required for Arp2/3 complex to nucleate polymerization [9] but appear to be absent from the cortex of yeast [11, 42]. We recognize other potential sources of mother filaments, including the possibility that Wsp1p/Las17p may nucleate actin filaments in patches [43].

Our hypothesis is an extension of a proposal that actin patches can provide mother filaments to initiate the assembly of an adjacent new patch through a "touch and trigger" mechanism [10]. Actin patches were observed to trigger actin filament assembly at a nearby site of endocytosis by direct contact. Although "touch and trigger" events were rare in wild-type cells, they were frequent in the *dip1* mutant, which has defects in nucleation of actin filaments in patches [10]. The "sever, diffuse, and trigger" mechanism can act over longer distances to explain actin assembly at sites of endocytosis physically separated from other actin patches. Our hypothesis does not preclude the possibility that the actin filament binding domains of adaptor proteins have separate roles at a later stage, after the assembly of actin patches, as suggested by studies in budding yeast [1, 41]. Indeed, our studies suggest that the TLD domain of End4p could complement the

ABD domain of Ent1p in a function separate from initiating the assembly of actin patches (Figure S4), perhaps coupling the actin filament network to the membrane of endocytic vesicles (step 5).

Simulations of actin patch dynamics [7] estimated that severing releases short actin filaments at a prodigious rate of ~30 per second from each >100 actin patches. The cytoplasmic concentration of actin in such fragments would rapidly reach the micromolar range, even if further severing and polymerization turn over the fragments in 10 s. A filament of 30 subunits has a translational diffusion coefficient of 5.2 $\mu m^2/s$ (see Experimental Procedures) and shorter fragments move even faster, so they diffuse rapidly throughout the cytoplasm. These short, rapidly diffusing filaments [7, 44] are difficult to distinguish from cytoplasmic actin monomers in cells with a small fraction of the total actin tagged with mGFP. Severing of filaments in actin cables nucleated by formin For3p may provide a second source of actin filament fragments [45].

Animal cells may also have small diffusing actin filaments that contribute to endocytosis. Fluorescence correlation spectroscopy (FCS) detected short (~80 subunits) actin filaments diffusing in the cortex of tissue culture cells [46], and electron microscopy of HeLa cells showed actin filaments associated with early endocytic invaginations that were not detected by correlated fluorescence microscopy [12]. Cofilin may generate these filaments, perhaps explaining how cofilin contributes to actin polymerization at the leading edge of animal cells [20].

Actin filament binding sites on adaptor proteins Pan1p and End4p are important to initiate actin nucleation in patches. The affinities of the APW motif of Pan1p and the TLD domain of End4p for actin filaments (K_d = ~3 μM) are higher than alpha-actinins (K_d = 20 μM), which bind actin filaments in physiological settings. Given 240 molecules of End4p and Pan1p on the tiny surface of a coated pit (12,000 nm^2, assuming a diameter of 50 nm [47]), the density of actin filament binding sites is 1/50 nm^2. This high density of actin filament binding sites on the cytoplasmic surface of a coated pit may favor multivalent binding of short filaments.

Why Are Actin Filament Severing and Actin Filament Binding by Adaptor Proteins Required to Terminate the Accumulation of Adaptor Proteins and Recruit NPFs?

Slow severing of actin filaments by cofilin and deletion of actin-binding sites from the adaptor proteins End4p and Pan1p cause similar defects, prolonged recruitment of both adaptors (step 3, Figure 6) at sites of endocytosis and delayed recruitment of the NPFs Wsp1p and Myo1p. Our experiments show that the actin filament binding sites on End4p and Pan1p are complementary, since deletion of both sites causes more severe defects than deletion of the individual sites. Interestingly, a budding yeast *pan1* mutant is synthetic lethal with a clathrin light chain (*clc1*) truncation mutant that is missing its *sla2*/*end4*-binding motif [48].

These features suggest that recruitment of actin filaments by adaptor proteins is part of a negative feedback loop that limits the accumulation of the adaptor proteins, as well as a positive signal for binding NFPs. Actin filaments are not required for adaptor proteins to concentrate at nascent sites of endocytosis, since both accumulate in the presence of LatA. However, nothing is known about how binding of actin filaments to these adaptor proteins provides negative feedback to limit their accumulation. Similarly, the LatA experiments showed that actin filaments are not required for Wsp1p to concentrate with the adaptor proteins at sites of endocytosis. Nevertheless, when severing is compromised or the adaptor proteins lack actin filament binding sites, Wsp1p binds only after the adaptor proteins have accumulated to much higher levels. Thus actin filaments must directly or indirectly favor Wsp1p binding.

On the other hand, LatA reduced the recruitment of both Myo1p and Arp2/3 complex and eliminated actin filament polymerization. Verprolin (Vrp1p) may recruit a small number of Myo1p molecules to patches by linking to Wsp1p [25], but direct interactions with actin filaments are likely to recruit most Myo1p to actin patches [25, 29]. Since Myo1p appears in patches prior to Arp2/3 complex [6, 24], the initial binding sites for Myo1p may be actin filament fragments bound to End4p and Pan1p.

Experimental Procedures

Fission Yeast Strains, Cell Culture, and Microscopy

Table S1 lists the strains used in this study. Standard yeast culture techniques were used. Cells were imaged with an Olympus IX71 microscope equipped with a confocal spinning-disk unit. The Supplemental Experimental Procedures provide details.

Construction of the adf1::GFP-adf1 Strain

We amplified the strong ADH promoter (Padh) sequence from fission yeast genomic DNA by PCR and subcloned it into the *pFA6a-KanMX6-41nmt1-mGFP* vector [49] in place of the *41nmt1* promoter. We amplified the KanMX6-Padh-mGFP fragment for targeting to the 5′ end of the endogenous *adf1* coding sequence by homologous recombination [49].

Tracking and Counting the Numbers of Fluorescent Fusion Proteins in Actin Patches

We tracked actin patches semimanually with ImageJ plug-ins. We selected actin patches in time-lapse fluorescence micrographs with maximum fluorescence intensities within the middle three slices of a five-slice z series. We measured the fluorescence intensity of each actin patch as the sum of the fluorescence in three slices within a circle with a diameter of 0.67 μM (five pixels), after subtracting the background cytosolic fluorescence, based on the fluorescence surrounding the patch. Final values of the fluorescence intensities of the patches were corrected for exposure time, camera noise, uneven illumination, and photobleaching [6, 31]. We converted the fluorescence intensities of actin patches into the numbers of mGFP fusion proteins with a standard curve based on the total cellular intensities of seven standard proteins [6, 24].

Protein Purification and Binding Assay

GST-Pan1$_{1633-1794}$ was expressed in *E. coli* and purified by passing through affinity, gel filtration, and ion exchange columns. GST-Pan1$_{1633-1794}$ was bound to actin filaments at room temperature and centrifuged at 213,300 × *g* for 40 min. For details, please see Supplemental Experimental Procedures.

Supplemental Information

Supplemental Information includes five figures, one table, Supplemental Experimental Procedures, and Supplemental Results and can be found with this article online at http://dx.doi.org/10.1016/j.cub.2013.05.005.

Acknowledgments

This work was supported by NIH research grant GM-025338 to T.D.P. The authors thank Julien Berro for providing ImageJ plug-ins and Rajesh Arasada for providing strains and for helpful discussions. The authors also thank Jian-Qiu Wu and Masaki Edamatsu for providing strains.

Received: December 14, 2012
Revised: April 2, 2013
Accepted: May 2, 2013
Published: May 30, 2013

References

1. Kaksonen, M., Toret, C.P., and Drubin, D.G. (2005). A modular design for the clathrin- and actin-mediated endocytosis machinery. Cell *123*, 305–320.
2. Newpher, T.M., Smith, R.P., Lemmon, V., and Lemmon, S.K. (2005). In vivo dynamics of clathrin and its adaptor-dependent recruitment to the actin-based endocytic machinery in yeast. Dev. Cell *9*, 87–98.
3. Aghamohammadzadeh, S., and Ayscough, K.R. (2009). Differential requirements for actin during yeast and mammalian endocytosis. Nat. Cell Biol. *11*, 1039–1042.
4. Weinberg, J., and Drubin, D.G. (2012). Clathrin-mediated endocytosis in budding yeast. Trends Cell Biol. *22*, 1–13.
5. Mooren, O.L., Galletta, B.J., and Cooper, J.A. (2012). Roles for actin assembly in endocytosis. Annu. Rev. Biochem. *81*, 661–686.
6. Sirotkin, V., Berro, J., Macmillan, K., Zhao, L., and Pollard, T.D. (2010). Quantitative analysis of the mechanism of endocytic actin patch assembly and disassembly in fission yeast. Mol. Biol. Cell *21*, 2894–2904.
7. Berro, J., Sirotkin, V., and Pollard, T.D. (2010). Mathematical modeling of endocytic actin patch kinetics in fission yeast: disassembly requires release of actin filament fragments. Mol. Biol. Cell *21*, 2905–2915.
8. Kaksonen, M., Sun, Y., and Drubin, D.G. (2003). A pathway for association of receptors, adaptors, and actin during endocytic internalization. Cell *115*, 475–487.
9. Mullins, R.D., Heuser, J.A., and Pollard, T.D. (1998). The interaction of Arp2/3 complex with actin: nucleation, high affinity pointed end capping, and formation of branching networks of filaments. Proc. Natl. Acad. Sci. USA *95*, 6181–6186.
10. Basu, R., and Chang, F. (2011). Characterization of dip1p reveals a switch in Arp2/3-dependent actin assembly for fission yeast endocytosis. Curr. Biol. *21*, 905–916.
11. Mulholland, J., Preuss, D., Moon, A., Wong, A., Drubin, D., and Botstein, D. (1994). Ultrastructure of the yeast actin cytoskeleton and its association with the plasma membrane. J. Cell Biol. *125*, 381–391.
12. Collins, A., Warrington, A., Taylor, K.A., and Svitkina, T. (2011). Structural organization of the actin cytoskeleton at sites of clathrin-mediated endocytosis. Curr. Biol. *21*, 1167–1175.
13. Martin, A.C., Welch, M.D., and Drubin, D.G. (2006). Arp2/3 ATP hydrolysis-catalysed branch dissociation is critical for endocytic force generation. Nat. Cell Biol. *8*, 826–833.
14. Chan, C., Beltzner, C.C., and Pollard, T.D. (2009). Cofilin dissociates Arp2/3 complex and branches from actin filaments. Curr. Biol. *19*, 537–545.
15. Andrianantoandro, E., and Pollard, T.D. (2006). Mechanism of actin filament turnover by severing and nucleation at different concentrations of ADF/cofilin. Mol. Cell *24*, 13–23.
16. Pavlov, D., Muhlrad, A., Cooper, J., Wear, M., and Reisler, E. (2007). Actin filament severing by cofilin. J. Mol. Biol. *365*, 1350–1358.
17. Maciver, S.K., Zot, H.G., and Pollard, T.D. (1991). Characterization of actin filament severing by actophorin from Acanthamoeba castellanii. J. Cell Biol. *115*, 1611–1620.
18. Chen, Q., and Pollard, T.D. (2011). Actin filament severing by cofilin is more important for assembly than constriction of the cytokinetic contractile ring. J. Cell Biol. *195*, 485–498.
19. Lappalainen, P., and Drubin, D.G. (1997). Cofilin promotes rapid actin filament turnover in vivo. Nature *388*, 78–82.
20. Ghosh, M., Song, X., Mouneimne, G., Sidani, M., Lawrence, D.S., and Condeelis, J.S. (2004). Cofilin promotes actin polymerization and defines the direction of cell motility. Science *304*, 743–746.
21. Okreglak, V., and Drubin, D.G. (2007). Cofilin recruitment and function during actin-mediated endocytosis dictated by actin nucleotide state. J. Cell Biol. *178*, 1251–1264.
22. Nakano, K., and Mabuchi, I. (2006). Actin-depolymerizing protein Adf1 is required for formation and maintenance of the contractile ring during cytokinesis in fission yeast. Mol. Biol. Cell *17*, 1933–1945.
23. Lin, M.C., Galletta, B.J., Sept, D., and Cooper, J.A. (2010). Overlapping and distinct functions for cofilin, coronin and Aip1 in actin dynamics in vivo. J. Cell Sci. *123*, 1329–1342.
24. Wu, J.Q., and Pollard, T.D. (2005). Counting cytokinesis proteins globally and locally in fission yeast. Science *310*, 310–314.
25. Sirotkin, V., Beltzner, C.C., Marchand, J.B., and Pollard, T.D. (2005). Interactions of WASp, myosin-I, and verprolin with Arp2/3 complex during actin patch assembly in fission yeast. J. Cell Biol. *170*, 637–648.
26. Lewis, M.J., Nichols, B.J., Prescianotto-Baschong, C., Riezman, H., and Pelham, H.R. (2000). Specific retrieval of the exocytic SNARE Snc1p from early yeast endosomes. Mol. Biol. Cell *11*, 23–38.
27. Engqvist-Goldstein, A.E., Kessels, M.M., Chopra, V.S., Hayden, M.R., and Drubin, D.G. (1999). An actin-binding protein of the Sla2/Huntingtin interacting protein 1 family is a novel component of clathrin-coated pits and vesicles. J. Cell Biol. *147*, 1503–1518.
28. Wendland, B., and Emr, S.D. (1998). Pan1p, yeast eps15, functions as a multivalent adaptor that coordinates protein-protein interactions essential for endocytosis. J. Cell Biol. *141*, 71–84.
29. Lee, W.L., Bezanilla, M., and Pollard, T.D. (2000). Fission yeast myosin-I, Myo1p, stimulates actin assembly by Arp2/3 complex and shares functions with WASp. J. Cell Biol. *151*, 789–800.
30. Lechler, T., Shevchenko, A., and Li, R. (2000). Direct involvement of yeast type I myosins in Cdc42-dependent actin polymerization. J. Cell Biol. *148*, 363–373.
31. Arasada, R., and Pollard, T.D. (2011). Distinct roles for F-BAR proteins Cdc15p and Bzz1p in actin polymerization at sites of endocytosis in fission yeast. Curr. Biol. *21*, 1450–1459.
32. Ti, S.C., Jurgenson, C.T., Nolen, B.J., and Pollard, T.D. (2011). Structural and biochemical characterization of two binding sites for nucleation-promoting factor WASp-VCA on Arp2/3 complex. Proc. Natl. Acad. Sci. USA *108*, E463–E471.
33. Coué, M., Brenner, S.L., Spector, I., and Korn, E.D. (1987). Inhibition of actin polymerization by latrunculin A. FEBS Lett. *213*, 316–318.
34. Ayscough, K.R., Stryker, J., Pokala, N., Sanders, M., Crews, P., and Drubin, D.G. (1997). High rates of actin filament turnover in budding yeast and roles for actin in establishment and maintenance of cell polarity revealed using the actin inhibitor latrunculin-A. J. Cell Biol. *137*, 399–416.
35. Morton, W.M., Ayscough, K.R., and McLaughlin, P.J. (2000). Latrunculin alters the actin-monomer subunit interface to prevent polymerization. Nat. Cell Biol. *2*, 376–378.
36. McCann, R.O., and Craig, S.W. (1997). The I/LWEQ module: a conserved sequence that signifies F-actin binding in functionally diverse proteins from yeast to mammals. Proc. Natl. Acad. Sci. USA *94*, 5679–5684.
37. Toshima, J., Toshima, J.Y., Martin, A.C., and Drubin, D.G. (2005). Phosphoregulation of Arp2/3-dependent actin assembly during receptor-mediated endocytosis. Nat. Cell Biol. *7*, 246–254.
38. Iwaki, T., Tanaka, N., Takagi, H., Giga-Hama, Y., and Takegawa, K. (2004). Characterization of end4+, a gene required for endocytosis in Schizosaccharomyces pombe. Yeast *21*, 867–881.
39. Duncan, M.C., Cope, M.J., Goode, B.L., Wendland, B., and Drubin, D.G. (2001). Yeast Eps15-like endocytic protein, Pan1p, activates the Arp2/3 complex. Nat. Cell Biol. *3*, 687–690.
40. Wesp, A., Hicke, L., Palecek, J., Lombardi, R., Aust, T., Munn, A.L., and Riezman, H. (1997). End4p/Sla2p interacts with actin-associated proteins for endocytosis in Saccharomyces cerevisiae. Mol. Biol. Cell *8*, 2291–2306.
41. Skruzny, M., Brach, T., Ciuffa, R., Rybina, S., Wachsmuth, M., and Kaksonen, M. (2012). Molecular basis for coupling the plasma membrane to the actin cytoskeleton during clathrin-mediated endocytosis. Proc. Natl. Acad. Sci. USA *109*, E2533–E2542.
42. Rodal, A.A., Kozubowski, L., Goode, B.L., Drubin, D.G., and Hartwig, J.H. (2005). Actin and septin ultrastructures at the budding yeast cell cortex. Mol. Biol. Cell *16*, 372–384.
43. Urbanek, A.N., Smith, A.P., Allwood, E.G., Booth, W.I., and Ayscough, K.R. (2013). A novel actin-binding motif in Las17/WASP nucleates actin filaments independently of Arp2/3. Curr. Biol. *23*, 196–203.
44. Young, M.E., Cooper, J.A., and Bridgman, P.C. (2004). Yeast actin patches are networks of branched actin filaments. J. Cell Biol. *166*, 629–635.
45. Martin, S.G., and Chang, F. (2006). Dynamics of the formin for3p in actin cable assembly. Curr. Biol. *16*, 1161–1170.
46. Gowrishankar, K., Ghosh, S., Saha, S., C, R., Mayor, S., and Rao, M. (2012). Active remodeling of cortical actin regulates spatiotemporal organization of cell surface molecules. Cell *149*, 1353–1367.
47. Kukulski, W., Schorb, M., Kaksonen, M., and Briggs, J.A. (2012). Plasma membrane reshaping during endocytosis is revealed by time-resolved electron tomography. Cell *150*, 508–520.
48. Boettner, D.R., Friesen, H., Andrews, B., and Lemmon, S.K. (2011). Clathrin light chain directs endocytosis by influencing the binding of the yeast Hip1R homologue, Sla2, to F-actin. Mol. Biol. Cell *22*, 3699–3714.
49. Bähler, J., Wu, J.Q., Longtine, M.S., Shah, N.G., McKenzie, A., 3rd, Steever, A.B., Wach, A., Philippsen, P., and Pringle, J.R. (1998). Heterologous modules for efficient and versatile PCR-based gene targeting in Schizosaccharomyces pombe. Yeast *14*, 943–951.